J Solid State Electrochem (2005) 9: 96–105
DOI 10.1007/s10008-004-0565-2

ORIGINAL PAPER

E. Shembel · R. Apostolova · V. Nagirny · I. Kirsanova
Ph. Grebenkin · P. Lytvyn

Electrolytic molybdenum oxides in lithium batteries

Received: 25 February 2004 / Accepted: 6 May 2004 / Published online: 16 July 2004

Abstract Nonstoichiometric molybdenum oxides (e-Mo_xO_y) were synthesized by cathodic reduction of aqueous ammonium and sodium molybdate solutions. Surface morphology of electrolytic (e) deposits, the chemical composition, crystal lattice structure, and the characteristics of electrochemical Li^+ intercalation for such synthesized oxides were determined by the cation composition of molybdate solution and the conditions of deposit annealing. The electrochemical intercalation of Li^+ ions in these Mo-oxides was investigated in thin-layer "ballast-free" electrodes, as a pasted composite cathode in lithium batteries, and as an anode in lithium-ion batteries, with liquid organic and polymer electrolytes. The reversible discharge capacity of e-Mo_4O_{11} synthesized from ammonium molybdate electrolyte in thin-layer ballast-free electrodes can exceed 225 mAh g^{-1} for more than 170 cycles.

Keywords Electrolytic oxides · Nonstoichiometric Mo-oxides · Cathode · Anode · Li^+-intercalation

Introduction

Increasing demand for small-size autonomous power sources raises the interest in thin-layer lithium batteries. Oxides of transient metals are suitable cathode materials for such batteries. From a great number of production methods for thin films of metal oxides, the technologically simple electrolysis method of aqueous solutions is very promising. This method allows sensitive control of the chemical composition, oxidation, and hydration degree of the electrolysis products. This was shown in the investigations devoted to the electrolytic synthesis of vanadium oxides [1, 2, 3]. By electrolysis we have produced vanadium oxides [4, 5] as well as sodium-vanadium oxide bronzes β-$Na_xV_2O_5$, (x = 0.22–0.40) [6, 7]. Electrolytic synthesis of binary oxides of Mn-Co [8], Mn-Ni, Ni-Co [9], carried out by us, obtained lithiated cathodic materials with increased columbic cycling efficiency—spinel structures $LiMn_{2-y}Me_yO_4$ (Me = Co, Ni, Cr and y = 0.1–0.5) and layered structures $Li_xCo_{1-y}Ni_yO_2$. This line of electrolytic oxide materials can be supplemented by molybdenum oxides. The use of thin electrolytic molybdenum oxide films for different electrochemical devices is well known [10, 11, 12, 13]. In [14] we have described the electrolytic synthesis of nonstoichiometric molybdenum oxide for lithium batteries.

The present publication is devoted to the investigations of physicochemical and structural properties and the surface morphology of thin-layer and powdered electrolytic deposits of molybdenum oxides. The electrochemical properties of these deposits were compared with those described in literature for molybdenum oxides MoO_3, MoO_2 and of nonstoichiometric composites $Mo_{18}O_{51}$, $Mo_{17}O_{47}$ as cathode materials in lithium batteries [15, 16]. The comparatively inexpensive trioxide MoO_3 has a high primary discharge capacity, but a lower discharge voltage as compared with V_2O_5 and MnO_2 [17]. Nevertheless, lithium batteries based on MoO_3 are competitive among other lithium batteries with solid-phase cathodes. A number of small-sized Li-MoO_3 batteries are already produced industrially [18].

During the discharge–charge process of reversible intercalation of lithium ions into the crystalline structure of MoO_3, lithium-molybdenum oxide bronzes are formed [19, 20, 21]. When during cycling the ratio Li/Mo exceeds 1.5 a lattice degradation and a decrease in discharge capacity are observed. This fact promoted a search of molybdenum oxides of nonstoichiometric composition with better electrochemical characteristics than those of stoichiometric oxides. Nonstoichiometric

E. Shembel · V. Nagirny · Ph. Grebenkin
Ener1, Ft. Lauderdale, FL 33309, USA

R. Apostolova · I. Kirsanova
Ukrainian State Chemical Technology University,
49005 Dnepropetrovsk, Ukraine

P. Lytvyn (✉)
Institute of Semiconductor Physics, Kiev, Ukraine
E-mail: shembel@onil.dp.ua

molybdenum oxides are characterized by some unique properties. Thus, the oxide $Mo_{17}O_{47}$ has a lower resistance (< 0.05 Ω cm) than other molybdenum oxides (≥1 Ω cm) [22]. The nonstoichiometric amorphous oxide $MoO_{2+\delta}$ ($\delta = 0.5$) has been recommended as anode material for lithium-ion batteries [10].

During lithium ion intercalation in nonstoichiometric molybdenum oxides, binary phases of the type $Li_{ny}Mo_mO3_{m-1}$ are formed. The specific discharge capacity of nonstoichiometric molybdenum oxides can exceed 0.4 mAh g^{-1} [23, 24, 25]. According to [24], among the nonstoichiometric oxides Mo_4O_{11}, $Mo_{17}O_{47}$, $(Mo_{0.92}V_{0.08})_5O_{14}$, and Mo_8O_{23} the oxide $Mo_{17}O_{47}$ has the highest intercalation cyclability. Its average discharge voltage is 1.85 V, and its reversible discharge capacity is 1.5 Li/Mo. Its theoretical specific energy (490 Wh kg^{-1}) is comparable to those of V_6O_{13} and TiS_2. The limiting values of the reversible lithium ion intercalation Li/Mo in oxides are: Mo_4O_{11} 1.62, Mo_8O_{23} 1.26, and Mo_9O_{26} 1.08 [26, 27]. Higher discharge characteristics have been obtained for the oxide Mo_8O_{23} [25]. Its discharge capacity in lithium batteries reaches 80 Ah kg^{-1} while discharging at a current density of 1 mA cm^{-2} up to a voltage of 2.0 V.

Experimental

Synthesis of electrolytic molybdenum oxides

The optimal conditions of electrolysis providing compact coatings of e-Mo-oxides with good properties have been determined earlier [14]. Based on these data the synthesis of e-Mo-oxides in the present investigation was carried out from solutions of ammonium or sodium molybdate.

In the case of deposition from an ammonium solution, a saturated (over an insoluble deposit) solution of $(NH_4)_6Mo_7O_{24}\cdot 4H_2O$ (Anala R quality) with a salt concentration of 320 g L^{-1}, and a pH value of 6.5–7.0 was used as a base electrolyte. The synthesis of e-Mo oxides from sodium molybdate solutions was performed using a solution of Na_2MoO_4 (420–450 g L^{-1}) as a base electrolyte.

The electrolysis of the aqueous molybdate solutions was performed in glass cells with a volume of 0.25 dm^3 at 80–85 °C. For cathode and anode, stainless steel plates were used with the area ratio $S_{cathode}:S_{anode} = 1:5$. Inoperative areas of the cathode were isolated by polyethylene coatings. The current density on the cathode was $I_{cathode} = 10$–15 mA cm^{-2}.

The quality of the oxide coating was estimated visually by the degree of uniformity and by its mechanical stability after a bending of 180°. Deposits of e-Mo-oxides were produced as a disperse powder as well as a compact film.

During electrolysis of molybdate solutions some parallel reactions can proceed simultaneously:

$$MoO_4^{2-} + 2H_2O + 2\bar{e} \rightleftarrows MoO_2 + 4OH^{-1} \quad (1)$$

$$2MoO_4^{2-} + 5H_2O + 6\bar{e} \rightleftarrows Mo_2O_3 + 10OH^{-1} \quad (2)$$

$$2MoO_4^{2-} + 3H_2O + 2\bar{e} \rightleftarrows Mo_2O_5 + 6OH^{-1} \quad (3)$$

The standard potentials of these reactions are close to 0.20–0.35 V [28]. The potentials of the actual beginning of molybdenum oxide formation indicate a significant value of overpotential for the corresponding reactions. This can be caused by the multistage reduction mechanism of the higher molybdenum oxide resulting in the formation of nonstoichiometric compounds.

The deposits of the e-Mo oxides were held at 18–20 °C and stored over P_2O_5. Then they were treated at 180–550 °C for different periods of time (the detailed conditions of thermal treatment are indicated for each particular case).

Investigation of e-Mo-oxides

X-ray diffraction analysis

Analysis was carried out on the device DRON−2.0 in Cu K_α−radiation by using powdered e-Mo-oxide samples.

Absorption IR spectra

Spectra were obtained with a spectrophotometer Specord-75IR in the spectral range $\nu = 4000$–500 cm^{-1} by using a KBr-matrix.

Thermal analysis

e-Mo-oxides were investigated using a derivatograph Q-1500 D at a sample heating rate of 10° min^{-1} with a standard of Al_2O_3. Sample mass was 200 mg .

Morphology

e-Mo-oxide surface was investigated using Digital Instruments Nanoscope IIIa.

Electrochemical characteristics

Electrochemical characteristics were determined in coin batteries of 2325 size with lithium anodes, and in 3-electrode sealed cells with an auxiliary lithium electrode and a reference Li/Li^+ electrode. e-Mo-oxides were also investigated in Li-ion batteries ($LiCoO_2$/e-Mo_8O_{23}). The cathode material ($LiCoO_2$) was synthesized by heating a dry mixture of $LiOH{*}H_2O$ and Co_3O_4. An X-ray diffraction analysis showed the presence of $LiCoO_2$ (about 99%) and traces of a nonidentified compound. An electrolyte PC + DME + 1 M $LiClO_4$ containing not more than 100 ppm of water was

used. Polymer electrolyte PVdF-CTFE (31508/1001 Solvay), EC, DMC (Merck) 1 M $LiPF_6$ (Merck) have been used in the batteries with ballast-free electrodes. Polymer films were formed on a glass sheet from a solution of the polymer, DMF (Angarsk Chemical Reagents Plant, Russia) and were activated in the solution comprising EC, DMC, and 1 M $LiPF_6$. The charge–discharge characteristics were plotted on a test bench with computer control and registration.

Results and discussion

Morphology of the electrolytic molybdenum oxide deposits

The cation composition of the molybdate electrolyte and the subsequent thermal treatment have a distinctive influence on the surface morphology of the molybdenum oxide deposits. Deposits from ammonium electrolytes are smoother and with less grain sizes than those obtained from sodium-comprising electrolytes (Fig. 1). They practically do not follow the pattern of the substrate, whereas deposits from sodium-containing electrolytes are markedly influenced by the support surface.

During the thermal treatment of e-Mo-oxides the intensive relaxation processes of mechanical stresses result in film cracking and peeling. On a film surface the nonuniform nets of cracks depending on the annealing conditions are visible with optical microscopes. On the surface of the oxide film, deposited from ammonium electrolyte and annealed at 260 °C, the ''valleys'' of 10 nm can be observed. They are probably connected with the presence of ammonium ions in the oxide, which are extracted during the thermal treatment and thus change the internal mechanical stresses in the film. The annealing temperature of the deposits significantly affects the structure of the oxides. AFM images of the samples synthesized from ammonium molybdate electrolytes show (Fig. 2) how, with increasing annealing temperature, the surface morphology changes from a fine-grained structure for nonannealed samples to a coarse-grained one (T_{anneal} about 450°C) and then to a block-structure (T_{anneal} 600 °C).

For untreated deposits the grain base has an ellipsoid form; the lateral sizes of the grains being from 7 to 35 nm and the heights from 0.5 to 5.0 nm. The surface roughness of untreated samples is in the range of about 10 Å–1.2 nm. After thermal treatment a trend of increasing grain sizes is observed (samples T = 450, 600 °C in Fig. 2). In the sample with T_{anneal} of 450 °C the grains have an oblong form with a width of 12–85 nm, a length of 60–350 nm, and a height of 5–25 nm. The surface roughness, within a 5×5 μm field, is 9 nm; roughness of a smooth section is 3 nm. The blocks in the samples with T_{anneal} of 600°C is, probably, the result of grain coagulation. The linear size of the blocks with a height of about 1000 nm changes from 250 to 1500 nm. The surface roughness is 140 nm.

An analysis of the histogram of grain distribution according to lateral sizes and heights gives the possibility of judging the nature of grain formation during cathodic deposition of the oxides (Fig. 3). It can be seen that more homogeneous deposits with a more definite crystallographic orientation are precipitated from ammo-

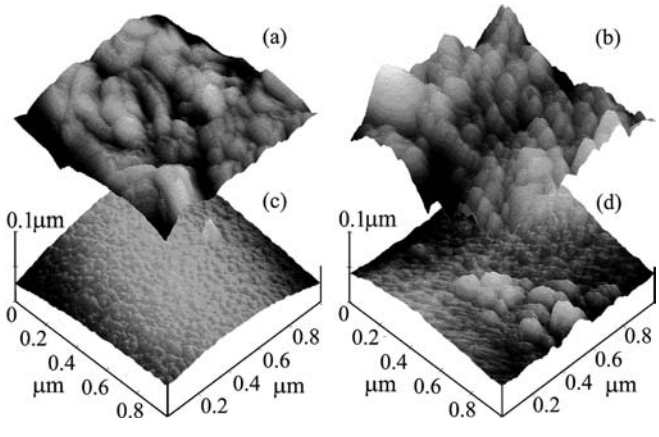

Fig. 1a–d AFM images of the deposit surface of e-Mo-oxides synthesized from the electrolytes containing Na^+ (**a**, **b**), or NH_4^+ (**c**, **d**). T_{treat}: 260 °C (**a**, **c**), 180 °C (**b**, **d**)

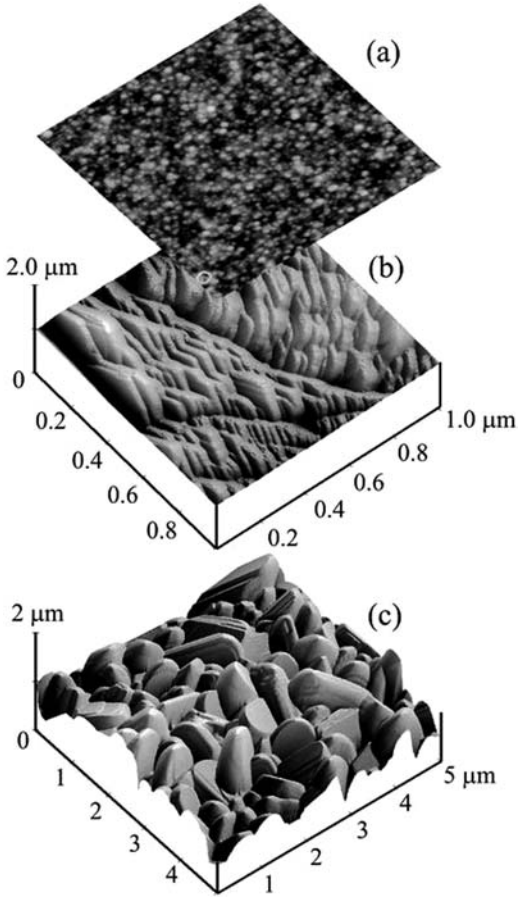

Fig. 2a–c AFM images of e-Mo-oxides obtained from NH_4-molybdate solution. T_{treat}: **a** 18 °C, **b** 450 °C, **c** 600 °C

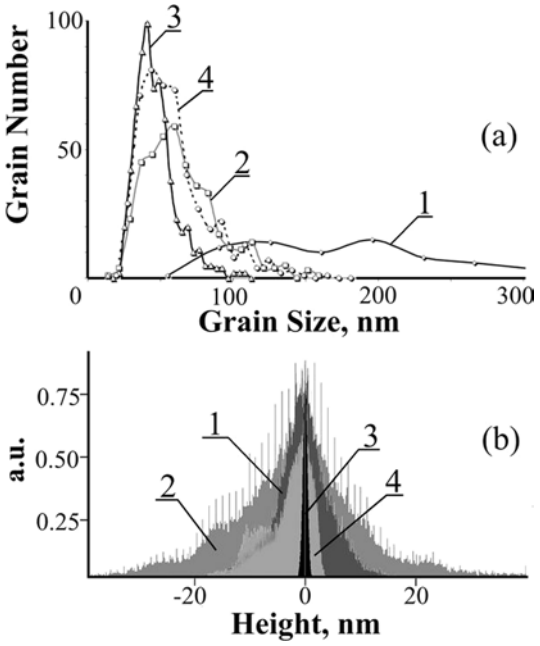

Fig. 3 Distribution histograms of **a** size distribution of grains in e-Mo-oxide deposits, **b** (*1–4*) height of the surface points of e-Mo-oxides. The oxides are synthesized from electrolytes comprising Na^+ (*1*, *2*), or NH_4^+ (*3*, *4*). T_{treat}: 260 °C (*1*, *3*), 180 °C (*2*, *4*)

nium molybdate solutions. Changes in the value of T_{anneal} influence the grain heights to a larger extent than the lateral grain sizes. It seems that moderate values of T_{anneal} are preferable for producing deposits with a higher specific surface.

For deposits obtained from sodium molybdate solutions a wide spread of grain sizes is typical (especially after treatment at 260 °C). This is probably due to a coarsening of the grains at higher temperatures and the tendency to reach a thermodynamic equilibrium. The histogram of peak distribution on the surface indicates a higher homogeneity of surface microstructure with uniform transition alteration between peaks and cavities, thus leading to a lower surface activity of the material, if deposited as a compact coating.

Based on the analysis of the morphological data, e-Mo-oxides with annealing temperatures ranging from 18 to 260 °C can be recommended for thin-layered cathodes in lithium batteries, obtained from NH_4-molybdate solution.

X-ray patterns of powdered e-Mo-oxides

X-ray patterns of the powdered e-Mo-oxide deposited from different solutions and with the different values of T_{anneal} are shown in Figs. 4 and 5. The results of the X-ray diffraction analysis of e-Mo-oxides are summarized in Table 1.

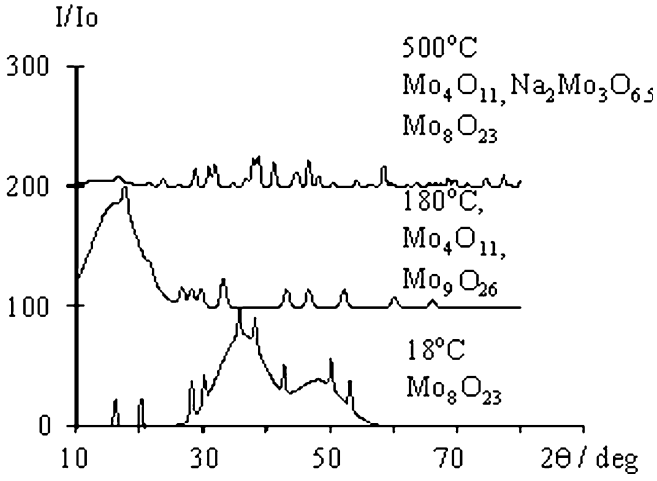

Fig. 4 X-ray patterns of e-Mo-oxides obtained from sodium molybdate solutions

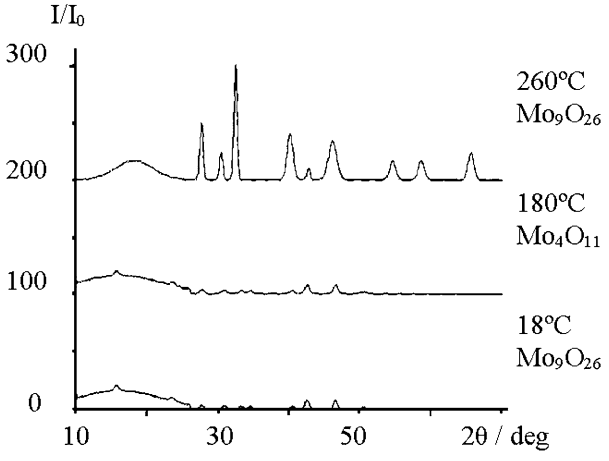

Fig. 5 X-ray patterns of e-Mo-oxides obtained from ammonium molybdate solutions

Judging by the data obtained, the electrolyte composition and annealing temperature of the deposits significantly influence the stoichiometry of the molybdenum oxide deposits and the crystallite size. The untreated deposits have a dark, close to black color. On the X-ray patterns of these samples the indistinct diffractional reflections of small intensity can be observed (Figs. 4, 5). The chemical composition of the oxides, obtained from ammonium and sodium molybdates is different. The crystallite size of the deposits grows with increasing intensity of the thermal treatment.

Crystallites synthesized from ammonium molybdate are more coarse than those obtained from sodium-containing solutions. Some differences in the composition of these oxides are observed after their annealing at 180 °C (7 h). Against a background of a wide halo the reflexes of Mo_4O_{11} are identified in oxides deposited from ammonium electrolytes. Deposits from sodium molybdate solutions include a continuous line of oxides from Mo_4O_{11} to Mo_9O_{26}.

Table 1 Results of the X-ray diffraction analysis of e-Mo-oxides for different synthesis conditions

Sample no	Electrolyte cation	T_{anneal}, τ °C (h, min)	Stoichiometry of oxide	Crystallite size nm
1	NH_4^+	18	Mo_9O_{26}	18.1
2	Na^+	18	Mo_8O_{23}	12.5
3	NH_4^+	180 (10h)	Mo_4O_{11}	21.5
4	Na^+	180 (10h)	Mo_4O_{11}–Mo_9O_{26}	21.1
5	NH^+_4	550 (5 min)	Mo_9O_{26}	32.3
6	NH_4^+	260 (7 h)	Mo_9O_{26}	68.4
7	NH_4^+	550 (70 min)	MoO_3	43.8
Krasny Khimik Plant, Russia			MoO_3	55.2
9	Na^+	500 (7 h)	$Na_2Mo_3O_{6.5}$ Mo_4O_{11}, Mo_8O_{23}	
10	Na^+	500(3 h)	Mo_8O_{23}, Na_4MoO_5	

The intensity of the thermal treatment influences both the crystallinity and the oxidation degree of the deposited molybdenum oxides. At a long, average-temperature exposure (260 °C, 7 h) an oxide is obtained with a composition similar to that after a high-temperature short-time exposure (550 °C, 5 min). A molybdenum oxide of the highest valency (MoO_3) has been produced after a high-temperature annealing (550 °C) of the deposit obtained from an ammonium electrolyte. From a sodium molybdate solution after annealing at 550 °C the following mixtures are formed: $Mo_8O_{23} + Na_4MoO_5$ (T_{anneal} 3 h) and $Na_2Mo_3O_{6.5} + Mo_4O_{11} + Mo_8O_{23}$ (T_{anneal} 5 h).

The presented results clearly show the ample opportunities for the electrolytic production of different non-stoichiometric molybdenum oxides.

IR absorption spectra of e-Mo-oxides

The IR spectra of oxides depend on the composition of the electrolyte and on the annealing temperature of the deposits. Spectra of e-Mo-oxides from ammonium molybdate solutions differ essentially from those obtained from sodium molybdate solutions (Fig. 6), indicating the significant role of the cation in the deposition electrolyte depending on the chemical composition of the deposited oxide.

Oxides from ammonium molybdate solution

The absorption spectra of these oxides depend on the annealing temperature. Absorption bands characterizing the oscillation of molybdenum-oxygen bonds ($\nu = 1000$–$500\ cm^{-1}$) (Table 2) in nonannealed e-Mo-oxides are different from those observed in molybdenum trioxide, produced by industrial chemical methods.

Peak values of the chemically synthesized MoO_3 sample (992, 868, and 866 cm^{-1}) correspond to the oscillation of the Mo = O-bond, in accordance with the data from literature for MoO_3 [12]: 990, 916, and 818 cm^{-1}. The wide absorption band 580 cm^{-1} is assigned to the oscillation bonds of O-Mo-O [29].

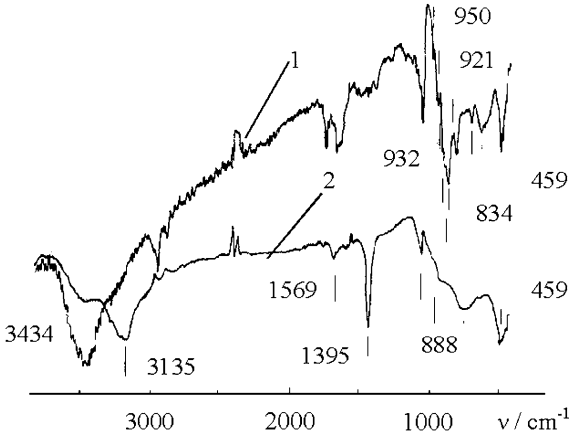

Fig. 6 Absorption IR spectra of electrolytic molybdenum oxides obtained from *1* sodium molybdate solutions, ammonium molybdate solutions *2*

With increasing annealing temperature an increase in the intensity of the band with the maximum 992–868 cm^{-1} and modification of the rest is observed as a result of O-Mo-O bond transformation into Mo = O. Peak intensity change (I, a.u.) relative to the intensity of the greatest peak in the 992–868 cm^{-1} range can be seen in Table 2 (nos. 6 and 7) . Rising annealing temperature also leads to the growth of a number of absorption bands. Presence of the absorption bands 3139 and 1400 cm^{-1} is a characteristic feature of the spectrum of nonannealed e-Mo-oxide from ammonium molybdate solutions. After annealing at temperatures above 180 °C they change. At 260 °C band 3139 cm^{-1} disappears, and intensity of the band 1400 cm^{-1} decreases. Further temperature increase promotes the disappearance of both bands. Their presence can be explained by inclusion in the deposit of NH_4^+ ions, which are decomposed by heating [12]. Deposits of e-Mo-oxides contain water, as is evidenced by the presence of a band near 3430 cm^{-1} (oscillation of the OH-bond) and 1630 cm^{-1} (deformation of H-O-H bonds) [30]. The result of a thermal treatment above 300 °C is a deformation and rearrangement of the chemical structure of e-Mo-oxides.

Table 2 Maxima of absorption bands on IR spectra of e-Mo-oxides obtained from ammonium molybdate solutions for different annealing temperatures of the deposit

No	*v*; *v*/I, a.u.					
	18 °C cm^{-1}	180 °C cm^{-1}	260 °C cm^{-1}	550 °C (15 min) cm^{-1}	680 °C (1.5 min) cm^{-1}	MoO_3 cm^{-1}
1	3439	3434	3434	3430	–	–
2	3139	3163	–	–	–	–
3	1569	1630	–	–	–	–
4	1395	1399	1399	–	–	–
5	1015	–	–	–	–	–
6	934; 37	947; 50	981; 54	988; 56	988; 66	992; 72
7	888; 51	893; 70	893; 84	868; 88	881; 90	868; 98
8	717	710	811	815	821	816
9	–	574	621; 513	620; 519	620	682
10	459	466	466	494	473	553
11	–	–	–	–	–	506

e-Mo-oxides from sodium molybdate solutions

Values of the maxima of absorption bands of e-Mo-oxides depending on temperature treatment are shown in Table 3.

It can be seen that the absorption spectra for deposits from sodium molybdate and from ammonium molybdate solutions are different (Table 3). A comparison of the data for deposits with an annealing temperature of 18 and 260 °C show that within this temperature range changes in the spectra are negligible. Only an intensity increase for the band near 900 cm^{-1} can be observed, indicating an ordering of the structure without its substantial rearrangement. A further increase of the annealing temperature up to 500 °C leads to an increase in the number of absorption bands and to an increase in their intensity. The most significant changes occur within the range 800–500 cm^{-1}. These changes can be tentatively explained by the formation of products of a thermochemical reaction between absorbed sodium ions and the molybdenum-oxygen skeleton of the oxide. The intercalation mechanism of sodium ions into the e-Mo-oxide was investigated by us and seems to be determined by the ion-exchange properties of the oxide, as is also the case for electrolytic vanadium oxides [31].

Table 3 Maxima of the absorption bands on IR spectra of e-Mo-oxides obtained from sodium-containing solutions for different annealing temperatures of the deposit

No	*v*			
	18 °C cm^{-1}	260 °C cm^{-1}	500 °C (3 h) cm^{-1}	500 °C (7 h) cm^{-1}
1	3434	3434	3434	3434
2	1630	1630	1630	1630
3	1015	–	1015	1015
4	940	941	968, 942	966, 932
5	919	922, 908	922, 909, 900	919, 906
6	879	881	874	893
7	866	864	860	867
8	834	834	826	825
9	784	780, 720	800, 773, 740, 700	800, 740, 713, 700
10	594	594	673, 600	653, 513, 500
11	459	466	453	466

Thermal analysis of e-Mo-oxides

Derivatograms of e-Mo-oxides synthesized from ammonium and sodium molybdates show differences.

e-Mo-oxides from sodium molybdate solutions

These samples held at 18–20 °C during heating up to 460 °C lose their mass in two stages (Fig. 7a). According to the data of thermogravimetric analysis, nonannealed e-Mo-oxide corresponds to the composition MoO_x nH_2O (x = 2.75–2.88, n = 1.33–1.38). The quantity of water weakly bonded with the oxide is estimated to be about 1 mole/mole of oxide. On the DTA curve several thermal effects can be distinguished. The Exo (410 °C) corresponds to the crystallization of the oxide. At temperatures above 460 °C mass of the sample increases, indicating the beginning of oxidation processes with a well pronounced Exo at 535 °C.

e-Mo-oxides from ammonium molybdate solution

Within the temperature range 200–400 °C the derivatogram of these oxides is essentially different from those of the oxides obtained from sodium molybdate solutions. Thus, on the DTA curve (Fig. 7b) there is an additional Endo section of mass loss (390 °C), which can be connected with the joint decomposition of NH_4^+-ions and phase transitions of nonstoichiometric molybdenum oxides. Near this section at 400–410 °C an Exo due to crystallization is superimposed. Unlike Fig. 7a, in Fig. 7b there are no thermal effects within the temperature range 520–530 °C. The difference between the derivatograms of e-Mo-oxides synthesized from ammonium and sodium molybdates are connected with the ion exchange properties of the oxides. In ammonium solutions NH_4^+-ions can be included in the e-Mo-oxide [30]. In accordance with TGA and X-ray data the composition of oxides from ammonium electrolytes corresponds to the formula Mo_4O_{11}*2.13H_2O* 0.13NH_3. The presence of thermal effects at 520–535 °C on the derivatogram of e-Mo oxides, deposited from sodium molybdate electrolytes can be explained by the

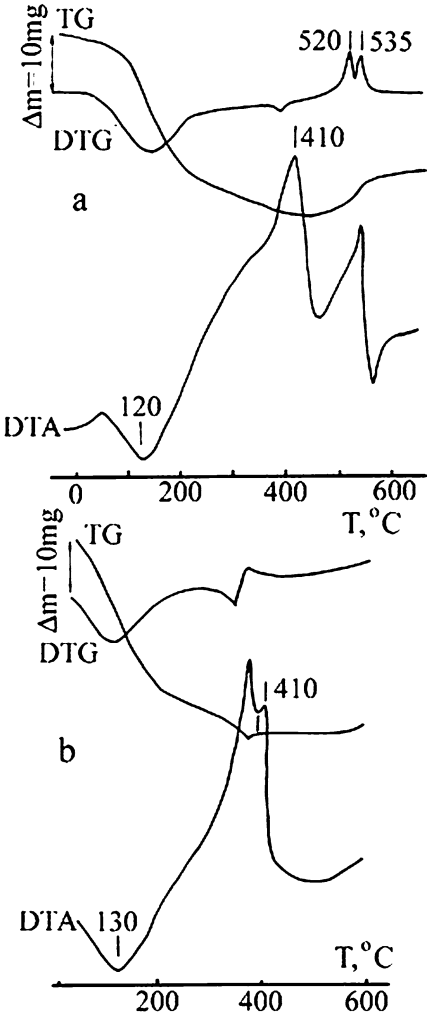

Fig. 7a, b Derivatograms of e-Mo-oxides **a** deposition from sodium molybdate solutions, **b** deposition from ammonium molybdate solutions

thermal chemical interaction of Na^+-ions included in the deposit with the molybdenum-oxygen skeleton.

Cathodic Li+ intercalation into e-Mo-oxides in liquid aprotic solution

Oxides from ammonium molybdate solutions

The open circuit voltage (OCV) of Li/e-Mo-oxide system is 3.25–3.55 V. The shape of the first galvanostatic discharge curve is determined by the annealing temperature of the oxide (Fig. 8). For nonannealed e-Mo-oxide the voltage changes gradually from 2.5 to 1.1 V. After annealing at 180–260 °C on the discharge curve the sections with different slopes appear. At annealing temperatures above 300 °C the discharge curve of e-Mo-oxide becomes similar to that of molybdenum trioxide with two horizontal voltage sections at 2.75–2.80 V and at 2.35–2.40 V.

The primary discharge capacity of e-Mo-oxide in thin-layer electrodes with the mass of 2–5 mg cm^{-2} reaches 240–340 mAh g^{-1} at discharge by a current density of 0.05 mA cm^{-2} up to a final voltage of 1.10 V. These values are lower than those obtained for pasted composite electrodes (Tables 4 and 5). Adhesion of e-Mo-oxide deposit to a substrate is an important factor determining discharge capacity.

During cycling, the discharge curve of e-Mo-oxide (180–300 °C) cathodes beginning from the second cycle "straightens" and becomes monotonous, without bends within the voltage range 2.5–1.1 V. The reversible discharge capacity of annealed e-Mo-oxides (180–260 °C) is higher than that of nonannealed ones.

In Fig. 9 the data for batteries based on e-Mo-oxide (T_{anneal} 180 °C, 10 h) are presented. During the 70th cycle the discharge capacity reaches 180–220 mAh cm^{-2} at discharge with a current density 0.1 mA cm^{-2} up to the final voltage 1.1 V. Under the same conditions

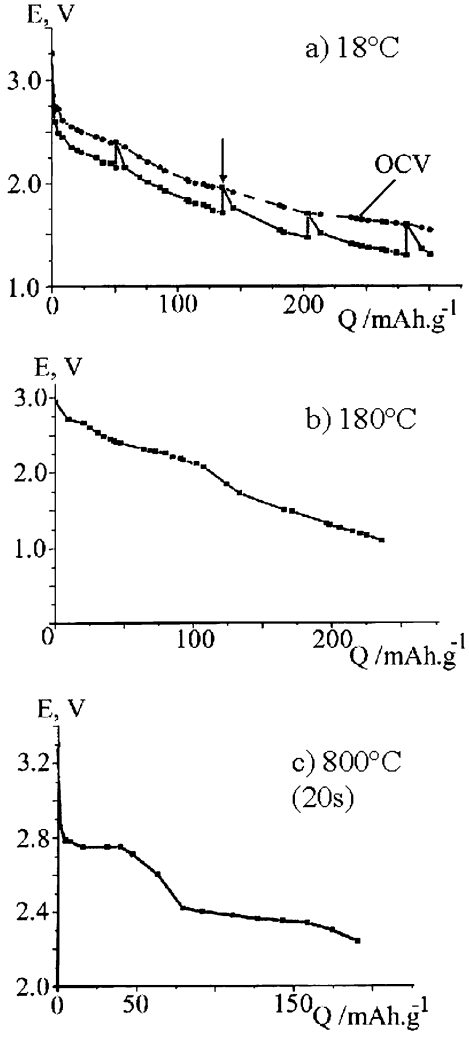

Fig. 8a–c Primary discharge curves of e-Mo-oxides obtained from NH_4-molybdate solutions depending on annealing temperature of the deposit in thin layer electrodes. Mass of e-Mo-oxides: **a** 2.79 mg, **b** 4.5 mg, **c** 26 mg

Table 4 Discharge cathodic capacity of 2325-size batteries based on e-Mo-oxide, obtained from an ammomium molybdate solution for different values of annealing temperature and the final discharge voltage (composite electrodes with 10–20 mg cm^{-2} of oxides, $I_{disch} = 0.1$ mA cm^{-2}, $I_{charge} = 0.05$ mA cm^{-2})

T_{anneal}	Q			
	$E_{disch}^{fin} = 1.5$ V		$E_{disch}^{fin} = 1.1$ V	
	1st cycle	10th cycle	1st cycle	10th cycle
°C	mAh g^{-1}	mAh g^{-1}	mAh g^{-1}	mAh g^{-1}
18			280–325	150–160
180	230–250	180–200	275–345	180–250
260	190–230	160–170	300–350	170–220

Table 5 Discharge cathodic capacity of 2325-size batteries based on e-Mo-oxides synthesized from an ammonium molybdate solution for different annealing temperatures; thin-layer "ballast-free" electrodes with mass 2–5 mg cm^{-2} ($I_{disch} = 0.1$ mA cm^{-2}, $I_{charge} = 0.05$ mA cm^{-2}, $E_{disch}^{fin} = 1.1$ V)

T_{anneal}	Q	
°C	1st cycle mAh g^{-1}	10th cycle mAh g^{-1}
18	240–320	140–160
180	240–340	150–250
260	255–320	140–200

stoichiometric molybdenum trioxide, produced by the "Krasny Khimik" plant (Russia) during the 10th cycle shows a lower capacity (≤ 170 mAh g^{-1}). During subsequent cycling this value decreases.

e-Mo-oxides deposited from sodium molybdate solutions

From this line of e-Mo-oxides the samples with annealing temperatures 18, 180, and 260 °C have been tested as cathodes in lithium batteries. The shape of the charge–discharge curves for the oxides from both sodium and ammonium molybdate solutions is similar. However, the specific discharge capacity and cycling efficiency of the products obtained from sodium molybdate solutions (Table 6) is lower than those obtained from ammonium molybdate solutions.

Electrochemical investigation of e-Mo-oxides as anode materials in lithium-ion batteries with liquid electrolyte

These investigations were performed in batteries of the type $LiCoO_2$/e-Mo_8O_{23}. The e-Mo-oxide deposited from a sodium molybdate electrolyte and held at a temperature of 18 °C was used as anode material.

The OCV of the battery $LiCoO_2$/e-Mo_8O_{23} is 0.035 V. This lithium-ion battery was cycled within the voltage range 3.30–0.90 V. In Fig. 10 the charge–discharge curve of the second cycle is shown. Over 10 cycles, the discharge capacity of the anode material reached 140–160 mAh g^{-1}.

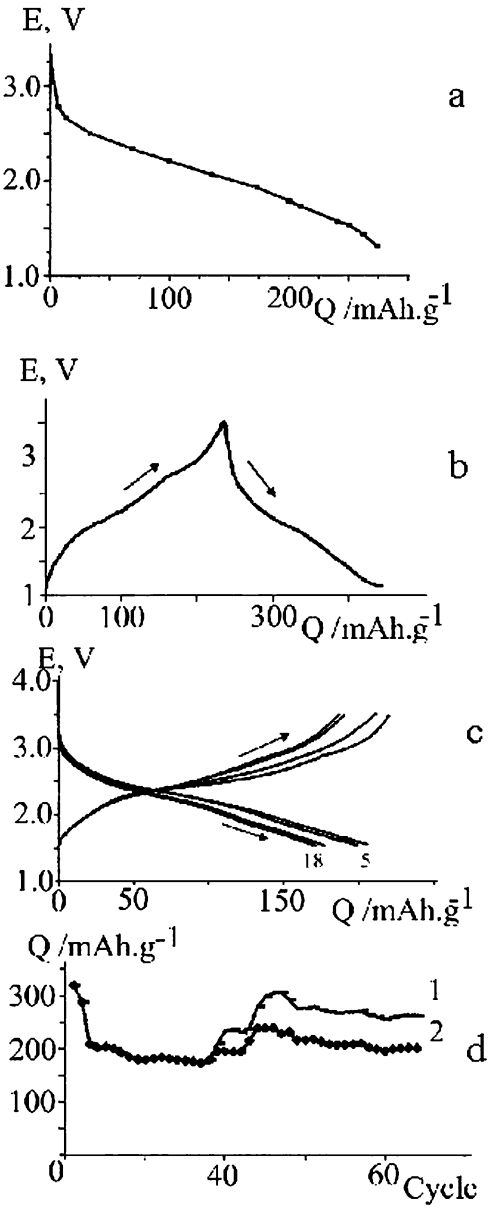

Fig. 9a–d Investigation results of e-Mo-oxide cathodes obtained from ammonium-containing electrolytes (T_{treat} 180 °C) in the 2325-size batteries: **a** first discharge, **b** charge–discharge curves at the 24th cycle. Mass of e-Mo-oxide is 9.9 mg, $I_{disch} = 0.2$ mA, $I_{charge} = 0.1$ mA. **c** Change of charge–discharge curves at cycling, **d** change of discharge capacity at cycling. For **c**, numbers near curves correspond to a cycle number. For **d**, final discharge voltage: 1.1 V for curve *1*, 1.5 V for curve *2*

e-Mo_4O_{11} in lithium batteries with polymer electrolyte (PE)

The OCV of the model Mo_4O_{11}/PE/Li reaches 2.98–3.23 V.

Mo_4O_{11} discharge–charge profile in the model for the 16th, 32nd, and 62nd cycles is shown in Fig. 11 (within cycling voltage of 2.8–1.1 V). The dependence of model discharge capacity on discharge current was investigated. Data are presented in Fig. 12.

Table 6 Discharge cathodic capacity of 2325-size batteries based on e-Mo-oxide obtained from sodium molybdate solution for different values of annealing temperature and final discharge voltage. Composite electrodes with an oxide mass 10–20 mg cm^{-2}, $I_{disch} = 0.1$ mA cm^{-2}, $I_{charg} = 0.05$ mA cm^{-2}

T_{anneal}	Q			
	$E_{disch}^{fin} = 1.5$ V		$E_{disch}^{fin} = 1.1$ V	
°C	1st cycle mAh g^{-1}	10th cycle mAh g^{-1}	1st cycle mAh g^{-1}	6th cycle mAh g^{-1}
18			250–260	160
180	200–210	125–150		
260	200–210	120–130		

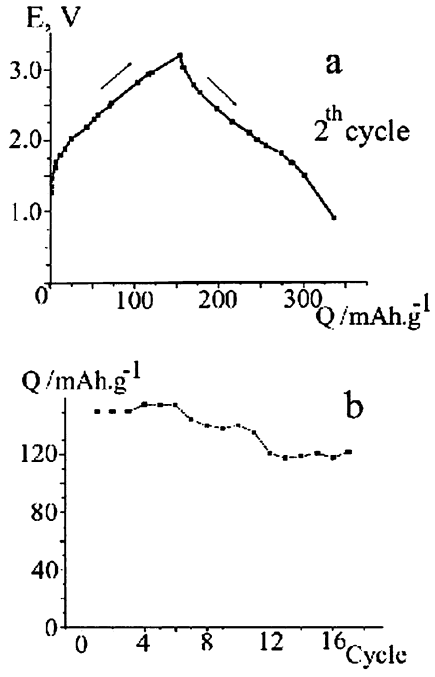

Fig. 10a, b Investigation results of the 2325-size batteries of the system $LiCoO_2/Mo_8O_{23}$: **a** charge–discharge curve, **b** change of the discharge capacity during cycling. T_{dry} 18 °C, mass of e-Mo-oxides is 8.12 mg, $I_{disch} = 0.2$ mA, $I_{charge} = 0.05$ mA

Discharge capacity of Mo_4O_{11}-oxide remains at above 200 mAh/g for more than 170 cycles at the discharge rate of 50–200 μA/g, at room temperature.

Mo_4O_{11}-oxide capable of effective reversible cycling within the voltage range 1.8–0.1 V as anodic material for lithium–ion batteries is shown in Fig. 13.

Conclusions

By the electrolysis of aqueous sodium and ammonium molybdate solutions a number of nonstoichiometric molybdenum oxides and sodium molybdenum oxide

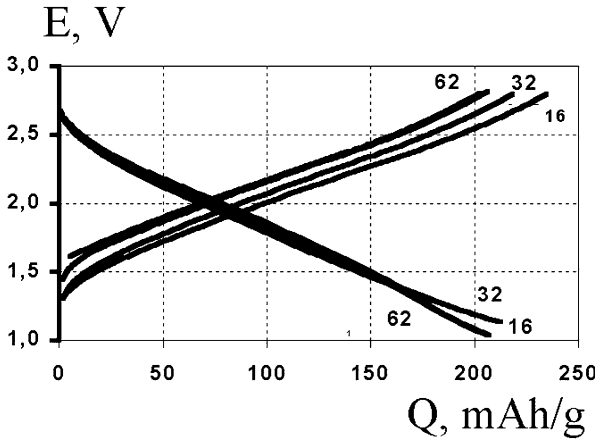

Fig. 11 Discharge–charge profile of Mo_4O_{11} in model Mo_4O_{11}/PE/Li as a cathode material for lithium batteries for the 16th, 32th, and 62th cycles. Mo_4O_{11} mass 1 mg/cm^2, $I_{disch} = 50$ mA/g, $I_{charge} = 30$ - mA/g

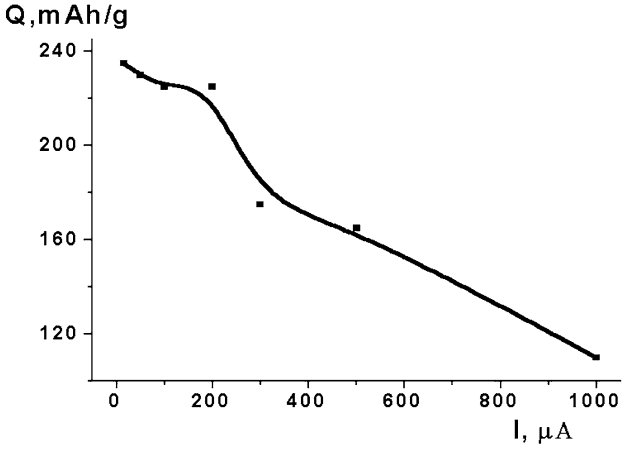

Fig. 12 Dependence of Mo_4O_{11} discharge capacity in model Mo_4O_{11}/PE/Li on discharge current

compounds have been synthesized. It has been shown that the structure of the crystal lattice, the chemical composition of the synthesis products, and the shape of their surface depend on the nature of the cation in the deposition solution and on the temperature of annealing deposits.

The reversible electrochemical intercalation of lithium ions in e-Mo-oxides was investigated in cathodes of lithium batteries and as anodes for lithium-ion batteries. The discharge capacity of electrolytic deposits in pasted composite cathodes at the first discharge reaches 330–350 mAh g^{-1} for a final discharge voltage of 1.1 V. The reversible discharge capacity of nonannealed samples of e-Mo-oxides is lower than that of the samples annealed at temperatures of 180–260 °C. The discharge capacity of e-Mo_4O_{11} oxide synthesized from ammonium molybdate solution (T_{anneal} 180 °C) in cathodes of lithium batteries is at least 180–220 mAh g^{-1} (E_{disch}^{fin}

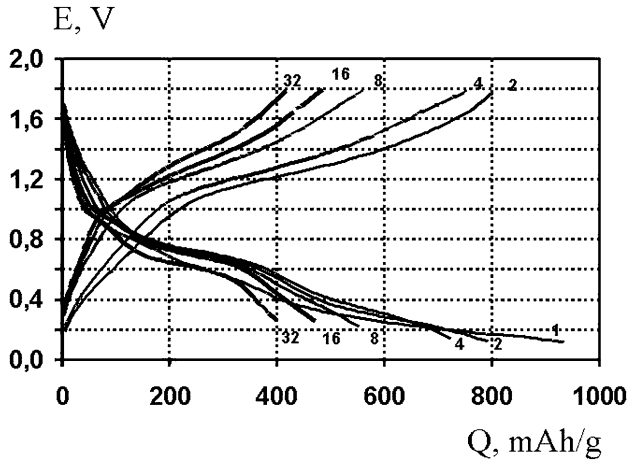

Fig. 13 Discharge–charge profile of Mo_4O_{11} in model Mo_4O_{11}/PE/Li as an anode material for lithium-ion batteries. Mo_4O_{11} mass 1 mg/cm^2, $I_{disch} = 50$ mA/g, $I_{charge} = 30$ mA/g

$= 1.1$ V, $I_{disch} = 0.1$ mA cm^{-2}). This is higher than the values for industrial samples of molybdenum trioxide under similar conditions. The reversible discharge capacity of e-Mo-oxides synthesized from ammonium molybdate solutions is higher than that for oxides from sodium molybdate solutions.

The loss of discharge capacity for e-Mo-oxides in ballast-free cathodes is due to a decreasing adhesion of the e-Mo-oxide deposits to the substrate during cycling. We tried to overcome these difficulties by using a polymer electrolyte in the batteries with ballast-free electrodes. The discharge capacity of thin layer e-Mo_4O_{11} in polymer electrolyte on the base PVdF-CTFE can reach more than 200 mAh g^{-1} at the 170th cycle.

Fundamental investigations of the behavior of e-Mo-oxides in lithium batteries with liquid organic electrolytes and with polymer electrolytes are under progress and will be submitted for publication soon.

Acknowledgements This research was supported by a grant from the Ministry of Science and Technology of Ukraine (contract #:42010190), a grant from the Scientific and Technology of Center Ukraine jointly with Dr. D. T. Meshri (ARC, USA)(project # 656), and a grant from the U. S. Civilian Research and Development Foundation jointly with Dr. P. Novak (Ener1, contract # USO-1207). The authors thanks sponsors for their financial support. The authors would like to thank a student M.Chuiko for her participation in the investigations concerning electrochemical intercalation of Li^+ in e-Mo-oxides.

References

1. Sato I, Asada T, Tokugava H, Kobayakawa K (1997) J Power Sources 68:674
2. Andrukaitis E, Bishenden E, Jacobs P, Lorimer J (1989) J Power Sources 26:475
3. Potiron E, Le Gal La Salle A, Verbaere A, Piffard G, Guyomard D (1999) Electrochim Acta 45:197
4. Apostolova R, Shembel E, Nagirny V (2000) Electrochemistry 36:41 (in Russian)
5. Shembel E, Apostolova R, Nagirny V, Aurbach D, Markovsky B (1999) J Power Sources 80:90
6. Apostolova R, Shembel E, Nagirny V, Aurbach D, Markovsky B (2000) Electrochemistry 36:695 (in Russian)
7. Shembel E, Apostolova R, Nagirny V, Aurbach D, Markovsky B (1999) J Power Sources 81–82:480
8. Apostolova R, Shembel E, Ubiykon V, Kvasha A, Baskevich A, Nagirny V (2000) J Questions Chem Chemtechnol 1:11 (in Russian).
9. Shembel E, Apostolova R, Nagirny V, Aurbach D, Markovsky B (2000) The 197th Meeting of Electrochem Soc, May 14–18, Toronto, Abstr 105
10. Manthiram A, Tsand C (1996) J Electrochem Soc 143:L142.
11. Kulusza P, Faulkner L (1988) J Amer Chem Soc 110:4905
12. Guerfi A, Painter R, Ado L (1995) J Electrochem Soc 142:3457
13. Liu S., Zhang O., Wang E., Dong Sh. (1999) Electrochem Commun 1:365
14. Nagirny V, Apostolova R, Baskevich A, Shembel E (2000) J Appl Chem 73:406 (in Russian)
15. Dampier F (1974) J Electrochem Soc 121:121
16. Margalit N (1974) J Electrochem Soc 121:1460
17. Kumagai N, Kumagai N, TannoK (1987) J Electrochem Soc 134:406
18. Nijnikovsky E (1998) J Electrochem 34:772 (in Russian)
19. Pasquali M, Pistoia G, Rodante (1981/82) J Power Sources 71:145
20. Wittingam M (1976) J Electrochem Soc 123:315
21. Wittingam M (1978) Progr Solid State Chem 12:41
22. Kihlborg L (1959) Acta Chem Scand 13:954
23. Icovim M, Panero S, Pistoia S, D'Agato A, Pistoia G, Temperoni C (1979) J Electroanal Chem 102:343
24. Christian P, Carides J, DiSalvo F, Waszczak J (1980) J Electrochem Soc 127:2315
25. Pistoia G, Temperoni C, Cignini P, Icovi M, Panero S (1980) J Electrochem Soc 109:169
26. Dines M (1975) Matter Res Bull 10:287
27. Murphy D, DiSalvo F, Carides J, Waszczak J (1978) Matter Res Bull 13:1395
28. Lurie Iu Iu (1979) The directory on analytical chemistry. Plenum, Moscow, p 480
29. Anwar M, Hogargh C, Bulpett R (1989) J Mater Sci 24:3087
30. Kumagai N, Kumagai N, Tanno K (1987) Electrochim Acta 32:1521
31. Apostolova R, Shembel E, Nagirny V, Aurbach D, Markovsky B, Koltipin Iu (2000) 6th Inter Conf ''Li Power Sources'', 19–21 September, Novochercask, p 62